

FILE COPY
NO. 3

FILE COPY
NO. I-W

**CASE FILE
COPY**

TECHNICAL MEMORANDUMS

NATIONAL ADVISORY COMMITTEE FOR AERONAUTICS

No. 461

CONTRIBUTION TO THE SYSTEMATIC INVESTIGATION

ON JOUKOWSKY PROFILES

By Gottfried Loew

From "Zeitschrift für Flugtechnik und Motorluftschiffahrt"
November 28, 1927

Washington
April, 1928

FILE COPY

To be returned to
the files of the National
Advisory Committee
for Aeronautics
Washington, D. C.

NATIONAL ADVISORY COMMITTEE FOR AERONAUTICS.

TECHNICAL MEMORANDUM NO. 461.

CONTRIBUTION TO THE SYSTEMATIC INVESTIGATION
OF JOUKOWSKY PROFILES.*

By Gottfried Loew.

This article resulted from the need of showing, in a simple way, how the aerodynamic properties of airfoils are affected by the shape of their profiles. No general solution of this problem could be found, since the profile shapes cannot ordinarily be expressed by simple mathematical formulas. This advantage is possessed only by the Joukowsky profiles and this discussion of the problem is therefore limited to them. Oskar Schrenk published in this magazine ("Zeitschrift für Flugtechnik und Motorluftschiffahrt," May 28, 1927, pp. 225-230) an article entitled "Systematische Untersuchungen an Joukowsky-Profilen" (For translation, see N.A.C.A. Technical Memorandum No. 422, "Systematic Investigation of Joukowsky Wing Sections"). (See also "Ergebnisse der Aerodynamischen Versuchsanstalt zu Göttingen," Report III.) The present investigation differs from the abovementioned one only in the form of presentation. The 74th and 79th reports of the D.V.L. ("Deutsche Versuchsanstalt für Luftfahrt") also relate to this work (N.A.C.A. Technical Memorandums Nos. 456 and 457).

To what extent the constants assumed by Martin Schrenk really

*"Ein Beitrag zur Systematik der Joukowsky-Profile" in "Zeitschrift für Flugtechnik und Motorluftschiffahrt," November 28, 1927, pp. 517-522.

hold good, can be readily learned from the diagrams.

The shape of a Joukowski profile is determined by the thickness parameter d/l and the camber parameter f/l . In the representation, one of the parameters was always assumed to be constant, while the other varied (Fig. 1). Diagrams were thus obtained for a thickness group $d/l = \text{constant}$ with variable camber or vice versa. The aerodynamic properties were represented by a function $c_a = f(c_w)$, $c_a = f(a)$, $c_a = f(c_w/c_a)$, or some similar one, according to the particular point of view. Hence there were three variables to be represented. This was done by plotting the values of f/l , in any desired scale, on the abscissas of a rectangular system of coordinates. The values of c_a were plotted on the axis of the ordinates. Obviously there is a point $P_1(c_{a1}, f/l_1)$ for each value of c_{wI} . In normal regions of like camber, i.e. with one and the same profile, the same c_{wI} value will occur with a different c_a value. Still another point $P_1'(c_{a1}, f/l_1)$ corresponds therefore to our c_{wI} value. In the case of a neighboring camber, the same c_{wI} , if it has a normal value, will appear in a similar manner at the points $P_2(c_{a2}, f/l_2)$ and $P_2'(c_{a2}', f/l_2)$. In this way, points can be found for the c_{wI} values in the field on the different parallels to the ordinate axis, each parallel indicating a camber and therefore a profile. All these points can then be connected by a curve, which shows how, with increasing camber, a constant c_w value occasionally coordinates with another c_a value. If

[illegible]

such curves, $c_w = \text{constant}$, be drawn for the most divergent values of c_w , there is produced what may be called a topographic map or diagram.

With this method of representation, we may speak of the curves $c_w = \text{constant}$ as lines of elevation or stratification. The curve of minimum drag surrounds the peak. The distance between the consecutive lines (the slope of the field) indicates the greater or less rapid increase in the drag, while the steep declivities indicate a separation of the flow. Sections through the field parallel to the axis of the ordinates give the polars for the camber or thickness represented on the abscissas. In this way intermediate profiles can be determined. The comparison of different charts representing individual thickness groups is more valuable and instructive.

The fundamental tendency of these fields is identical. They have a certain longitudinal axis, along which the intervals between the curves of constant c_w reach their maximum. From a spatial viewpoint, the most gradual slope of the drag field lies on this axis. In this direction the increase in the profile drag, with increasing c_a , is the smallest. The inclination of this axis is about the same for all fields. The boundary curves for the $c_{a \text{ max}}$ of each profile likewise approximately coincide for thin, thick and very thick profiles ($d/l = 0.10, 0.15, 0.20$). The thin profile remains about $c_a = 0.2$ behind the others. The lift increase of a profile is therefore predominantly a function

of its camber and its influence is in fact greater in thin profiles than in thick ones. The lower region is practically covered for nearly all profiles. The minimum profile drag for the thin profile lies at $c_a = 0$ and $f/l = 0$ and shifts with increasing thickness to about $c_a = 0.45$ and $f/l = 0.05$. For $d/l = 0.05$, the absolute coefficient of drag is $c_{wp} = 0.065$. For $d/l = 0.2$, $c_{wp} = 0.12$, which is nearly 100% worse.

For lack of space, only a few pages of the whole report can be published here, so that only a few of the examples can be given. Likewise some of the diagrams must be omitted, which were drawn for one and the same profile group, both for the simple profile drag and for the total drag of the Göttingen airfoil sections.

Figure 2 shows the profile-drag coefficients for a thin profile covering all the cambers investigated. The fundamental tendency of the field is a very stable and steady one, probably due somewhat to the influence of the few available data. Since the field has a sharp ridge and steep slopes, the profiles show a very good optimum, but a very small good region. The separation takes place very uniformly both in the upper and in the lower region.

Quite a different picture is presented by Figure 3, which applies to profile thicknesses much used on engine-driven airplanes. They have a convenient constructional thickness, without

being too thick. The field has a very unstable character. The $c_{a \max}$ is very high and climbs very rapidly with small cambers, but slower with large cambers. The separation processes are very abrupt in the lower region for ordinary profiles, but are more gradual for larger cambers. The minimum forms a distinct peak around the origin or zero point, but a flatter minimum is developed again over profile 580. It is obvious that the data for profile 541 were affected by some disturbance, since the whole field is distorted. I have heard that this was due to imperfections in the model. Furthermore, a symmetry of the polars of the symmetrical profile ($f/l = 0$) is to be expected.

Figure 4 represents a rectification of field 10. Despite the surprising uniformity, only a few measurements were made. The values of the profile 429 were arranged symmetrically with respect to the origin. Measurements with profile 541 were omitted, since they were unreliable. Lastly, care was taken that the intervals between the curves diminished uniformly, which is a necessary condition for a steady course of the polars. A negative camber denotes an inverted airfoil of positive camber, which is measured in the normal direction. The field was plotted only for values up to $c_{wp} = 0.02$. The corrections from subsequent check tests, the results of which are given in the third report of the Göttingen A.V.A. ("Ergebnisse der Aerodynamischen Versuchsanstalt zu Göttingen, 3 Lieferung"), greatly improve the field of departure 13.

Figure 5 was plotted for different thicknesses with the same camber. The field is to be regarded as a vertical section through the superposed camber fields. It shows a somewhat improved character. The $c_{a \max}$ is hardly affected by the thickness. The lower region, however, is favorably affected by the thickness. The minimum c_{wp} coefficient is obtained with thin airfoils.

Figures 6 and 7 afford a comparison of the moment coefficients in theory and in practice. In the third Göttingen report, already referred to, the theoretical formulas are so transformed, with the aid of a numerical table, that the theoretical calculations can be made for a perfectly definite Joukowski profile.

On the basis of such a table, the Göttingen investigators plotted theoretical lines of moment in their polar diagrams. The fields of practical and theoretical values were both plotted for the thickness $d/l = 0.1$. The camber appears again on the abscissa and the lift coefficients on the ordinate, while lines of constant-moment coefficients appear in the field. The Göttingen theoretical lines of moment were taken as the basis for plotting the theoretical moment field. The curves themselves were calculated, however, for the profiles 545 and 431. It was found, as also at Göttingen, that straight lines occur for small cambers, while curved lines are developed for large cambers. The location of the points is affected by the slightest inaccuracies in calculation. The tendency of the field in the region undisturbed

by separation phenomena is the same. In the region of separating flow and at $c_a = 0$, the value of c_m is indeterminate. Since the separation phenomena in the lower region for the most part proceed very slowly, unstable conditions develop in the practical field. There is agreement in the numerical values only for low-cambered profiles.

In addition to the simple relations between lift and drag and lift and wing moment, the gliding coefficient c_w/c_a and the climbing coefficient $c_w/c_a^{1.5}$ are of interest to the constructor in his aerodynamic calculations. Corresponding fields were therefore plotted for these values, both for the pure profile values and for the assumptions of a particular example. Figures 8 and 9, respectively, represent a field for the gliding coefficient and for the climbing coefficient of the thickness group $d/l = 0.1$ with an aspect ratio $t/b = 1/5$ and a structural-drag coefficient $c_{wr} = 0.03$. It is apparent that the gliding coefficients gradually fall from the best value both with increasing and with decreasing c_a values, while the climbing coefficients, after passing the maximum, fall very rapidly with increasing c_a values.

From such curves the constructor can obtain a very good idea of the effect of varying the camber and also of varying the thickness in corresponding fields. If he selects, for example, in the fields 3, 8, 9, a particular profile and then changes his choice by taking a larger or smaller f/l ratio, he can im-

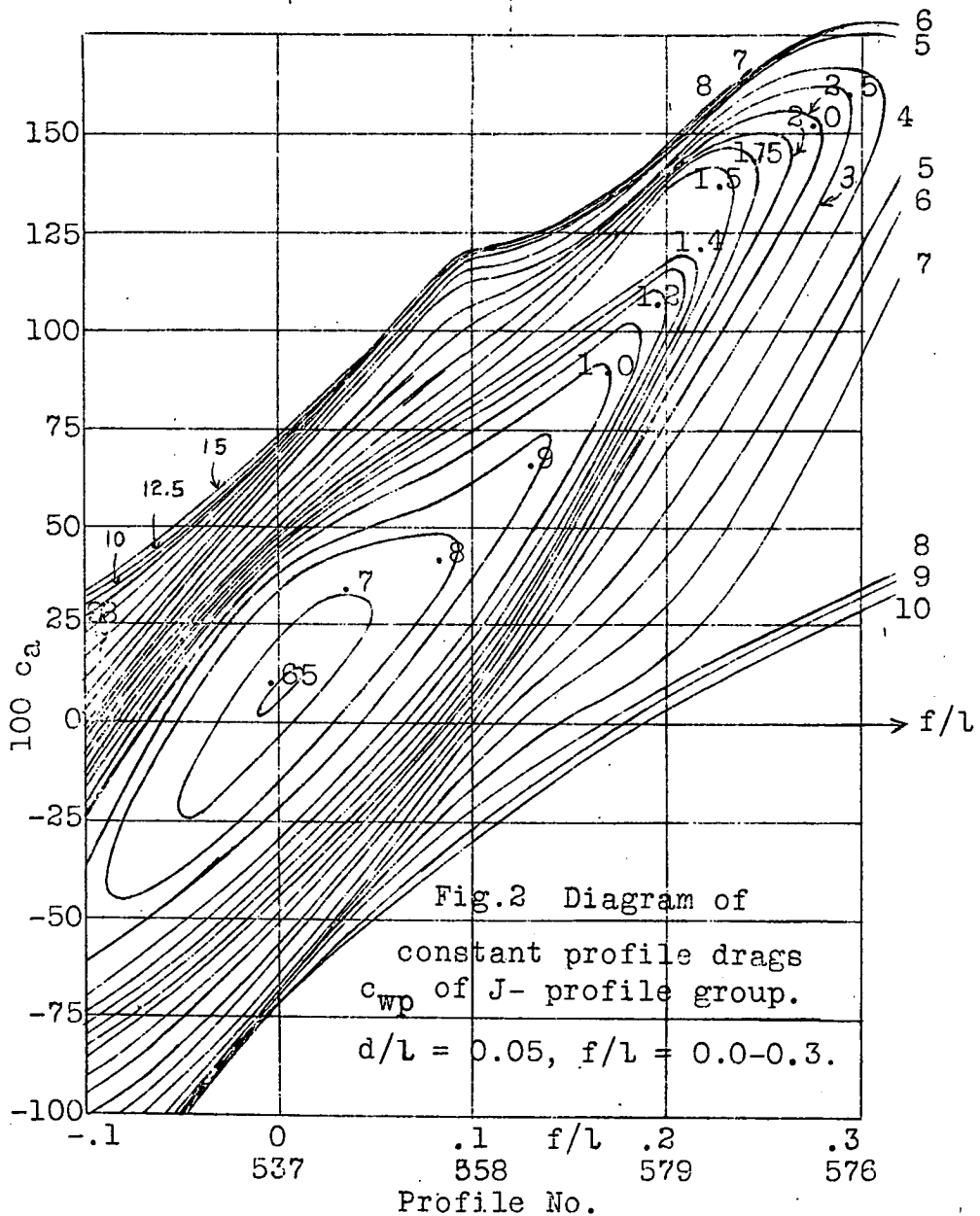
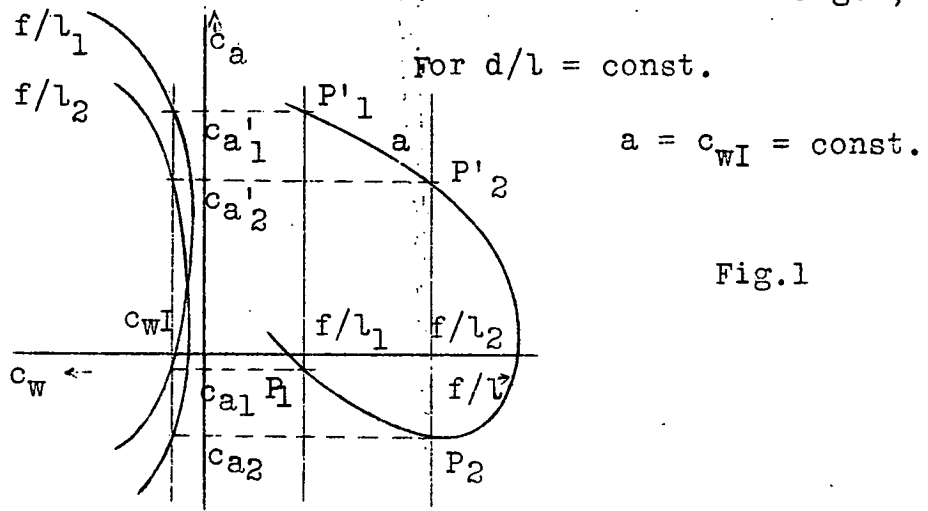
mediately see the effect of such changes. The practical range varies from $f/l = 0.07$ to 0.017 . The $c_{wi} + p_{min}$ varies thereby from 0.0115 to 0.032 and the $c_{a \max}$ increases from 1.25 to 1.5 , while the gliding coefficient remains constant. The climbing coefficient gradually increases and then decreases. For airplanes built for speed, greater variations can be made toward the axis of symmetry, but the climbing coefficient becomes noticeably poorer. Conversely the climbing coefficient is fairly good up to $f/l = 0.27$ and c_a increases to 1.7 , while the coefficient of glide rapidly grows poorer and $c_{w \min}$ decreases to 0.076 . It should be remembered that profile thickness has very little effect. In any case it has much less effect than the camber. These curves afford valuable data for researches on variable camber wings. Further discussion of these problems falls outside the scope of this article, since their thorough discussion would necessitate a very exact investigation of the whole problem, both in its aerodynamic and its constructive aspects.

In commenting on these results, it may be said that the fields are sufficiently consistent. This means that the results are good, especially in consideration of the very great distorted scale. Difficulties first arise in the region of incipient separation, due to the very unstable condition of flow. The only profile which gave bad results throughout was No. 541, as already mentioned. The discrepancies between its old and new measurements are indicated by dotted lines (Fig. 3). The curves repre-

sent the purely experimental results and leave the rectification to the reader.

In the graphic method, it is probable that the interpolations will also give sufficiently accurate results.

Translation by
National Advisory Committee
for Aeronautics.



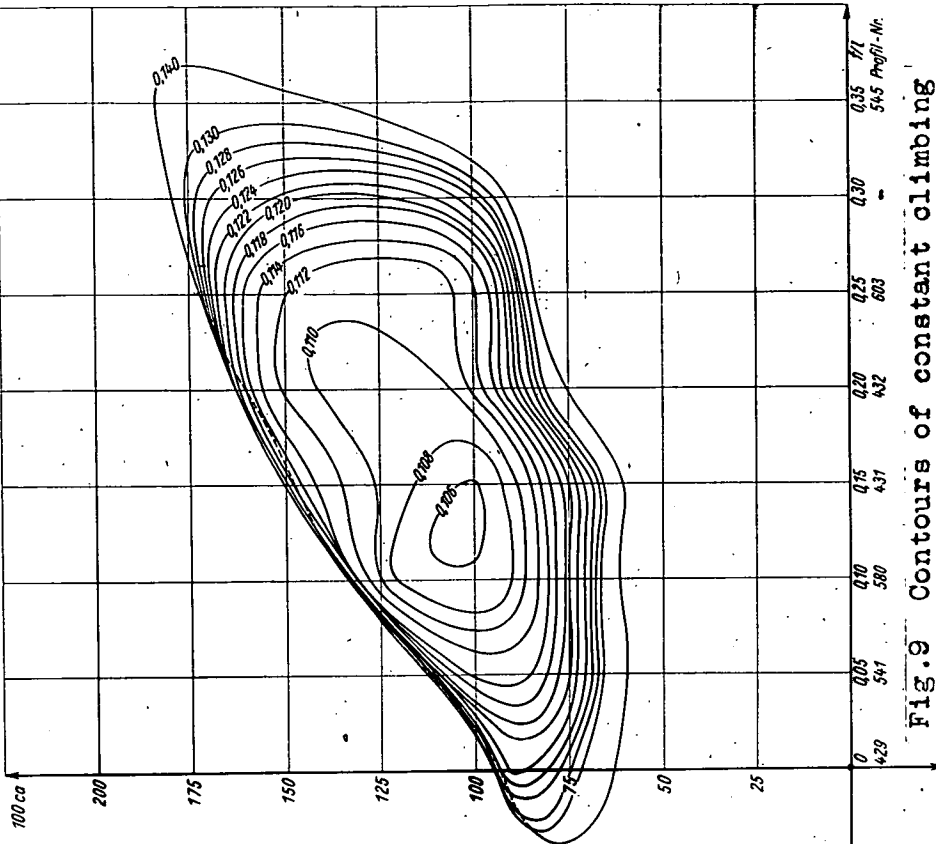


Fig.9 Contours of constant climbing coefficients $c_w + c_{w1} + c_{wI}$ at

$$\lambda = \frac{1}{5} \text{ and } c_{wI} = 0.03 \quad c_a$$

of the J-profile group. $d/l=0.1$, $f/l=0.0-0.35$.

(not rectified)

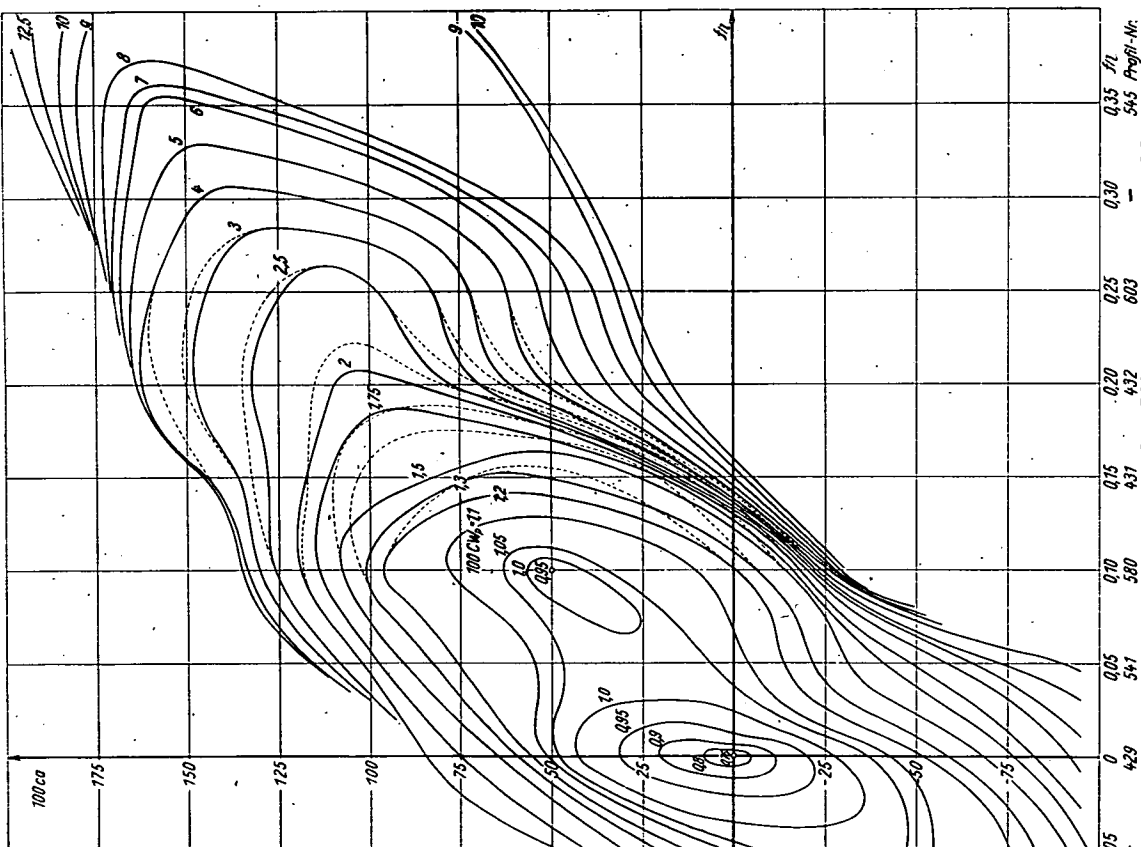
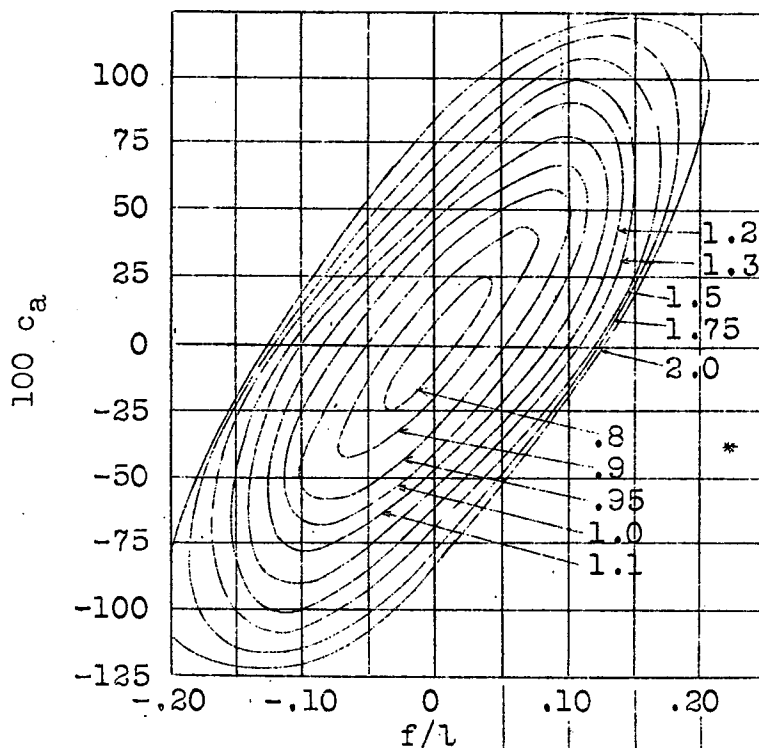


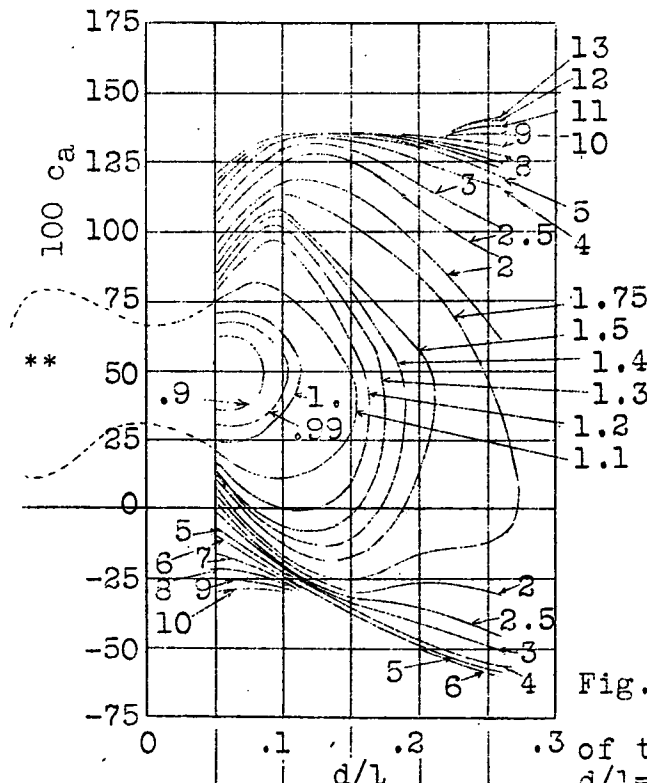
Fig.3 Diagram of constant profile drags of J-profile group. The dotted lines give results of new measurements.



* 429 rectified symmetrically with reference to the origin. 541 disregarded, because very irregular. dc_{wp}/dc_a constantly increasing.

Profile No. 429 541 580 431 432

Fig.4 Corrected chart of constant profile drags of the J-profile group. $d/l=0.1, f/l=0.0-0.35$.



** Example of an assumed course in the negative region. The negative thickness ($-d/l$) corresponds to the positive thickness ($+d/l$) according to the formula $\frac{d_1}{l} = \frac{1}{l/d-2}$ (for $\cos \gamma = 1$).

Fig.5 Chart of constant profile drags of the J-profile group. $d/l=0.1, f/l=0.0-0.35$

Profile No. 558 580 433 434 435

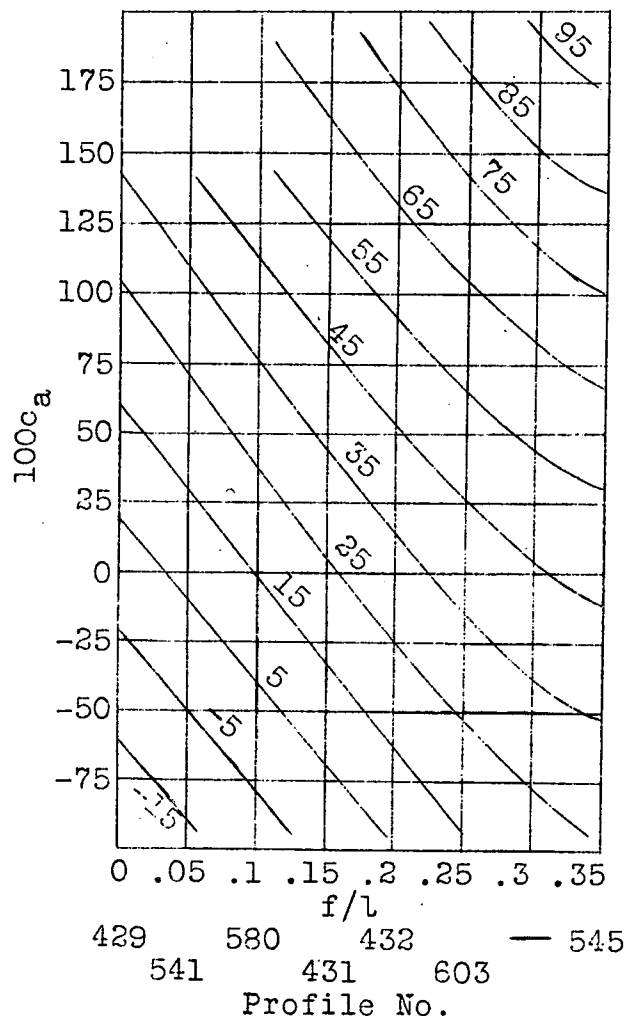


Fig.6 Diagram of constant theoretical c_m of J profile group. $d/l=0.1$, $f/l=0.0-0.35$

